

NUMERICAL MODELLING AND THERMAL SIMULATION OF PHASE CHANGE MATERIALS WITH ESP-R

Heim D¹ and Clarke J A²

¹ Department of Building Physics and Building Materials, Technical University of Lodz,
90-924 Lodz, Poland⁰

² Energy Systems Research Unit, University of Strathclyde, Glasgow, G1 1XJ, Scotland

ABSTRACT

The aim of the presented work is to refine the ESP-r system by incorporating phase change materials (PCM) modelling. The behaviour of PCMs is modelled using ESP-r's *special materials* facility. The effect of phase transition is added to the energy balance equation as a latent heat generation term according to the so-called effective heat capacity method. Numerical simulations were conducted for a multi-zone, highly glazed and naturally ventilated passive solar building. PCM impregnated gypsum plasterboard was used as an internal room lining. The air, surface and resultant temperatures were compared with the no-PCM case and the diurnal latent heat storage effect was analysed.

INTRODUCTION

At the present time many designers are attempting to utilise innovative technologies to achieve low energy design solutions. Because of the inherent complexity, modelling and simulation is required to arrive at optimal parameter values and avoid technology conflict. The work reported in this paper was concerned with the modelling of phase change materials to create a heavyweight response as a contribution to passive solar design.

It is well known that the thermo-physical properties of the construction materials will have a strong influence on a building's energy consumption. Within a passive solar design, the heat capacity of the inner wall layer is dominant. Traditional heavyweight constructions can give rise to problems of excessive thermal mass and cost. Where traditional building materials are combined with an inner PCM layer, isothermal phase change can be employed to provide close space temperature control at acceptable cost. Effectively, the additional latent heat of fusion is used to increase the thermal capacity of the construction.

Theoretical (Drake *et al* 1987, Peippo *et a.* 1991) and experimental (Athienitis *et al* 1997, Heim *et al* 2001) analyses of the optimal transition temperature and latent heat capacity of PCM structures have been reported. These data can be introduced to numerical simulations to enable an assessment of the diurnal

latent heat storage effect and so determine the expected savings in energy consumption. The storage effect of different PCM configurations may then be analysed for the specific context parameters. Few building simulation programs had refined PCM models at the commencement of the present work, the main objective of which was to modify the existing ESP-r program (Clarke 2001) to include phase-change phenomena. This would make it possible to model and simulate advanced active or passive building elements incorporating PCMs arbitrarily located within a multi-layered construction.

PCM – GYSPUM COMPOSITE

Thermal energy is generally stored as sensible or latent heat. In the former case the temperature of the medium changes during charging or discharging of the storage, whereas in the latter case the temperature of the medium remains more or less constant since it undergoes a phase transformation. Benard *et al* (1985) have presented an experimental comparison of latent and sensible heat within thermal walls.

The utilisation of PCMs in active and passive solar buildings has been a subject of interest since their first reported application in the 1940s (Lane 1983). Any PCM composite will comprise two components: a chemical, organic or inorganic compound that undergoes a phase transition within some desired operating temperature range, and a porous structure that acts as a containment for the heat storage substance. In a building context, pure organic or inorganic PCMs can be impregnated into the porous structure of traditional construction materials such as gypsum, concrete or ceramic, which are normally used as an internal surface lining. The thermal performance of different organic (e.g. paraffins, fatty acids *etc*) and inorganic (e.g. salt hydrates) chemical compounds have been analysed (Abhat 1983, Hawes *et al* 1993, Romanowska and Jablonski 1995), with the results demonstrating that organic materials are more thermally stable and easier to encapsulate.

Laboratory measurements of ceramic compounds with fatty acids were undertaken using a Differential Scanning Calorimeter method (Romanowska and Jablonski 1995). The results showed that it is

possible to obtain heightened heat accumulation with almost isothermal change of phase in the melting temperature range from 13.7°C to 33.3°C and the heat of phase change from 11.1kJ/kg to 82.4kJ/kg. The PCM considered here was self-nucleating, chemically stable and exhibited no overheating or overcooling effect.

MATHEMATICAL MODEL

The heat transfer processes in the PCM structures are complex, especially when the chemical compound is in the transition stage. During the phase change process (melting or solidification), the PCM encapsulated in a porous building material can exist in three states: solid, liquid and ‘mushy’ (two-phase). Additionally, the thermal properties of a matrix of construction material are different from the constituent properties. To simplify the mathematical model, the following assumptions were made:

1. The PCM-gypsum composites are treated as a body of uniform equivalent physical and thermal properties—principally specific and latent heat, density and thermal conductivity.
2. The heat transfer process across the PCM-gypsum board is considered as one-dimensional.

The differential equations of transient heat conduction with variable thermo-physical properties is given by:

$$\frac{\partial}{\partial t} \rho(T) h(T) = \nabla \cdot \left[\lambda(T) \nabla T(\vec{r}, t) \right] + g(\vec{r}, t) \quad (1)$$

where T is temperature, ρ density, h enthalpy, λ conductivity and g heat generation rate. When

$$\frac{\partial \rho}{\partial t} \approx 0 \quad \text{and} \quad \frac{\partial h}{\partial t} = \frac{\partial h}{\partial T} \frac{\partial T}{\partial t} = C_{eff}(T) \frac{\partial T}{\partial t}$$

equation (1) becomes:

$$\begin{aligned} \rho(T) C_{eff}(T) \frac{\partial T(\vec{r}, t)}{\partial t} = \\ = \nabla \cdot \left[\lambda(T) \nabla T(\vec{r}, t) \right] + g(\vec{r}, t) \end{aligned} \quad (2)$$

where C_{eff} is the effective heat capacity.

For the non-linear problem (in the phase change temperature range) defined by equation (2), the Goodman transform (Samarskii and Vabishchevich 1995) can be used to remove the temperature dependent, effective heat capacity, C_{eff}, outside the differential operator by defining a new dependent variable:

$$v = \int_{C_s}^{C_l} C_{eff}(T) dT$$

where C_s is the heat capacity in solid phase, and C_l the heat capacity in liquid phase.

Equation (2) can thus be rearranged:

$$\begin{aligned} \rho(T) C_{eff}(T) \frac{\partial T}{\partial v} \frac{\partial v}{\partial t} = \\ = \nabla \cdot \left[\lambda(T) \frac{\partial T}{\partial v} \nabla v \right] + g(\vec{r}, t) \end{aligned} \quad (3)$$

NUMERICAL MODEL

The ESP-r control volume approach was adapted to describe the physical elements of the PCM model using ESP-r’s zones and networks elements. This method also allows the adoption of variable thermophysical properties (Nakhi 1995). Spaces, described by geometry, construction and operational data, are interconnected using network models that describe any air and moisture flowpaths. The complete numerical model, together with boundary conditions and imposed control, is then passed to a central solver.

The control volume formulation is obtained by integrating associated partial differential equation (2) over a small polyhedron control volume V, applying the mean value theorem and divergence theorem, with homogeneous material and uniform boundary at each surface. Equation (2) thus becomes:

$$\rho(\bar{T}) C_{eff}(\bar{T}) V(\bar{T}) \frac{\partial \bar{T}}{\partial t} = -\lambda_s(T) \frac{\partial T}{\partial n_s} + V(\bar{T}) \bar{g} \quad (4)$$

where \bar{T} is the average temperature of V, g the heat generation rate over the control volume and n_s the outward drawn normal unit vector.

Heim (2002) presented some initial applications of the effective heat capacity method within ESP-r.

IMPLEMENTATION IN ESP-R

According to the control volume and the effective heat capacity method, the effect of the phase transition is added to the energy balance equation via material property substitution. Effective capacity is a highly non-linear function of temperature within the phase change temperature range. It can be substituted, however, by a linear relationship. Such an approach has been proposed for the thermal simulation of single PCM components (Drake 1987, Jokisalo *et al.* 2000).

Within ESP-r, PCMs was modelled using the concept of *special materials* (Kelly 1998). Special materials were introduced to ESP-r as a means of modelling active building elements that have the ability to change their thermo-physical properties in response to some external excitation (e.g. electro-chromic glazings). The special material functions of ESP-r may be applied to a particular node within a multi-layer construction. Any node defined as a special material is then subjected to a time variation in its basis thermo-physical properties.

PROBLEM DEFINITION

Within a building energy system, the most important feature of a PCM composite is its thermodynamic properties: melting point, transition temperature range and latent heat of phase change. The properties of the PCM-gypsum composites used in the work reported here are given in Table 1.

Table 1. Properties of PCM-gypsum composite.

MATERIAL PROPERTY	VALUE
latent heat of phase change [kJ/kg]	45.00
phase change temperature range [K]	1.00
conductivity [W/m ² K]	0.35
density [kg/m ³]	1000.00

Three, naturally ventilated, zones were established to represent a middle portion of a multi-storey office. The perspective view presented in Figure 1 shows the superimposed natural ventilation scheme. Two symmetrical zones are separated by a third, centrally placed, buffer zone.

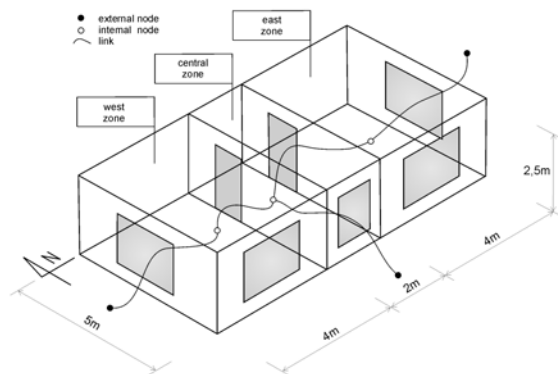


Figure 1. View of the 3 zones PCM building model.

Passive solar buildings, with their large glazing areas, may give rise to thermal discomfort problems. Different strategies such as controlled blinds, passive cooling or additional thermal mass may be used to mitigate the problem. Within the present study, additional thermal mass is achieved through the application of PCM impregnated gypsum board. The storage of latent heat increases the thermal capacity of the construction, allowing it to store solar energy while maintaining near constant temperatures.

Table 2. West and east zones description.

ZONE PARAMETER	VALUE
total volume [m ³]	50.00
floor area [m ²]	20.00
external opaque area [m ²]	16.50
external transparent area [m ²]	6.00
total PCMs wallboard area [m ²]	57.00
floor area / PCM wallboard area [-]	0.35
thickness of PCM panel [m]	0.012

Table 2 lists the describing parameters of the two main zones.

The thermo-physical properties of the partitions and the magnitude of the air flows were defined according to best practice guidelines. All external walls were constructed from 25cm of massive, concrete slab isolated with 12cm polystyrene from the outside. The heat transfer coefficient for all external, opaque partitions was set to 0.30W/m²K; and 1.3W/m²K for windows.

Weather data for Warsaw (52°N) in 1982 was used to define the boundary condition for the simulations. This year corresponds to the hottest summer between 1976 and 1985. The average ambient air temperature from July to September is 19.24°C and the total solar radiation is 1144.5MJ/m². The period from the beginning of the March to the end of November was selected for the analysis. The wind speed and direction determined the infiltration air flow through the openings, the magnitude of which were set to guarantee effective air flow rates in order to maintain the zone temperature not higher than 3K over the ambient temperature. The casual gains from equipment, lights and occupants were set to zero in order to remove their impact on the results and so make the results interpretation easier. Continuous heating corresponding to a fixed zone air temperature set-point of 20°C was defined.

First, simulations were conducted for the building without PCM-composites. Initial calculations showed that maximum resultant temperature recorded in the west zone was 33,6°C and 31,8°C in the east zone. Additionally, the overheating effect was noticed from 15th of June to 15th of September when internal temperatures exceeds 25°C during the day and night.

Now, an interior lining made from 1.2cm of gypsum PCMs-composite wallboard was applied to all surfaces except the floors in the west and east zones. Based on the resultant temperature history obtained from the initial simulation, the melting temperature (T_m) was set to 21, 24, 27 and 30°C. The solidification temperature (T_s) was assumed to be 1K higher than the melting point (i.e. 22, 25, 28 and 30°C respectively). Each composite has the same value of latent heat of fusion given by 45kJ/kg.

NUMERICAL ANALYSIS

A 15 minutes time step was used within both simulations. The values of the resultant temperature, PCM node temperature and latent heat of phase change were saved at each time step. To aid the analysis, the histories of these parameters were presented in weekly time periods. Each period was chosen to correspond to a different value of the melting temperature and contains the beginning of the phase change (i.e. where the wallboard's surface

temperature exceeds the melting temperature). The selected periods were:

$T_m = 21^\circ\text{C}$ – 6-12 March

$T_m = 24^\circ\text{C}$ – 27 March to 2 April

$T_m = 27^\circ\text{C}$ – 23-29 May

$T_m = 30^\circ\text{C}$ – 19-25 July.

The history of the PCM composite's surface temperature and internal node temperature compared with traditional gypsum board are presented. Figures 2, 5, 8, 11 represents surface temperatures for different values of the melting temperature. The internal surface is highly exposed to daily temperature fluctuation and direct solar radiation. The phase change process inside the wallboard allows a portion of the solar energy to be stored as latent heat. The surface temperature is about 0.5-1.0K lower than for the case of a zone with no PCM-gypsum composites. This result is due to the relatively wide (~1K) phase change temperature range, in comparison to the daily zone temperature fluctuation (~2K). The internal face of the wallboard (Figures 3, 6, 9 and 12) is thermally stable and the temperature is constant at the level of the assumed melting temperature. A more pronounced temperature fluctuation is seen for the ordinary material, where the node temperature varies more than 1K during 24 hours.

Figures 4, 7, 10 and 13 show the history of the latent heat flux during transition periods. Over a day the heat flux is positive and solar energy is stored in the material (melting process). The heat is released during the night when the zone's resultant temperature drops below the solidification temperature (solidification process). After a few weeks the phase change phenomenon ceases, the wallboard is completely loaded and unable to store more heat (Figure 18). The solar energy accumulated in the material is equal to the maximum latent heat of phase change. The first type of PCM-gypsum composite, with a melting temperature equal to 21°C , stores solar energy during March and releases it in November. From April to October the PCM panel is overloaded because the temperature is higher than the solidification temperature. The second type of composite, with a melting temperature equal to 24°C , works similarly. However, now the loading period lasts two months and the material is overloaded for only about four months. The third material ($T_m=27^\circ\text{C}$) does not exceed the fully loaded state, while the fourth material ($T_m=30^\circ\text{C}$) works periodically but does not seem to be useful for the case studied here.

The thermal behaviour of the wallboards also affects the room's resultant temperature. Figures 14 - 17 show the profiles over selected periods. An analysis

of these data does not show significant differences in the zone's performance. This derives from the relatively small thickness of the wallboard and the low latent heat of phase change (45kJ/kg). Another problem is that, from a practical point of view, the floor cannot be covered with a PCM-composite and therefore its surface heated rapidly and this had a significant impact on the room resultant temperature.

The results of numerical analysis confirmed the correctness of the method. The histories of the zone's resultant temperature and the wallboard's surface temperature show the influence of the phase change transition and the effect of latent heat storage. Comparative analyses with pure gypsum plasterboards show the advantages of latent heat, low temperature storage systems, and seem to indicate promise for the future.

CONCLUSIONS AND FUTURE WORK

This study is the first step in the integration of latent heat storage materials within a building structure. The initial model, implemented in ESP-r, to calculate the effect of phase change performed as expected but further refinements are required. The obtained results show the effect of latent heat storage on the thermal behaviour of the building. This effect did not cause a considerable reduction in diurnal temperature fluctuation. However, it did decrease the internal air temperature in the transitions periods when the solar energy was effectively stored. The PCM-gypsum composite designed for passive solar heating works properly under spring-autumn weather conditions and allows the stored energy to be utilised at the beginning of the heating season. However, to design the appropriate material properties for passive heating during winter, and cooling during summer, a wider analysis using multicriterion optimisation is planned. The behaviour of the material composite corresponds to the experimental measurements; further macro-scale experiments are necessary to validate the model. Additionally, a more accurate description of the PCM structure with variable density and conductivity will be analysed in the future.

ACKNOWLEDGEMENTS

This work was financed by the State Committee for Scientific Research from funds in 2002 – 2003 as a research project no. 5 T07E 021 23.

REFERENCES

- Abhat, A. 1983. Low temperature latent heat thermal energy storage: heat storage materials. *Solar Energy*, Vol. 30, No. 4: 313-332.
- Athienitis, A.K. & Liu, C. & Hawes, D. & Banu, D. & Feldman, D. 1997. Investigation of the thermal performance of a passive solar test-room

- with wall latent heat storage. *Building and Environment*, Vol. 32, No. 5.
- Benard, C. & Body, Y. & Zanolli, A. Experimental comparison of latent and sensible heat thermal walls. *Solar Energy*, Vol. 34, No. 6: 475-487.
- Clarke, J.A. 2001. *Energy simulation in building design, 2nd edition*. Oxford: Butterworth-Heinemann.
- Drake, J.B. et al. 1987. *PCMSOL – simulation code for a passive solar structure incorporating Phase Change Materials, Report ORNL – 6359*. Oak Ridge National Laboratory.
- Hawes, D. W. & Feldman, D. & Banu D. 1993. Latent heat storage materials. *Energy and Buildings*, Vol. 20: 77-86.
- Heim, D. 2002. Modeling building elements with the application of phase change materials. *Proceeding of 4th Ph.D. Symposium in Civil Engineering, P. Schiebl et al. (ed.), vol. 1*, Munich: 248-255.
- Heim, D. & Romanowska, A. & Jablonski, M. 2001. Zastosowanie kompozytów gipsowych modyfikowanych materiałem fazowo - zmiennym do akumulowania energii cieplnej w okresach temperatur umiarkowanych. *Proceeding of XV International Scientific and Technological Conference, Ekomilitaris-2001*, Zakopane: 172-179, (in Polish).
- Jokisalo, J. & Lamberg, P. & Siren, K. 2000. Thermal simulation of PCM structures with TRANSYS. *Proceeding of 8th International Conference on Thermal Energy Storage, TERRASTOCK-2000*, Stuttgart, Germany.
- Kelly, N.J. 1998. *Towards a design environment for building integrated energy systems: the integration of electrical power flow modeling with building simulation, PhD Thesis*. University of Strathclyde, Glasgow.
- Lane, G. A. 1983. *Solar Heat Storage: Latent Heat Materials, Vol.1*. CRC Press, Boca Raton, Florida.
- Nakhi, A.E. 1995. *Adaptive construction modelling within whole building dynamic simulation, PhD Thesis*. University of Strathclyde, Glasgow.
- Peippo, K. & Kauranen, P. & Lund, P.D. 1991. A multicomponent PCM wall optimized for passive solar heating. *Energy and Buildings*, Vol. 17: 259-270.
- Romanowska, A. & Jablonski, M. & Klemm, P. 1998. Kompozyt ceramiczny o podwyższonej akumulacji ciepła. *Proceeding of IV Polish Scientific and Technological Conference "Energodom '98"*, Krakow: 164-171 (in Polish).
- Samarskii, A.A. Vabishchevich, P.N. 1995. *Computational Heat Transfer, volume 1 Mathematical Modelling*. John Wiley & Sons.
- Telkes, M. 1978. Trombe wall with phase change storage material. *Proceeding of II National Passive Solar Conference*, Philadelphia: 283-287.

NOMENCLATURE

A brief description of the symbols used in your paper.

T – temperature [°C]

ρ – density [kg/m³]

h – enthalpy [J/kg]

λ – conductivity [W/m K]

g – heat generation rate

C_{eff} – effective heat capacity [J/kg °C]

C_S – heat capacity in solid phase [J/kg °C]

C_l – heat capacity in liquid phase [J/kg °C]

T_m – melting temperature [°C]

T_s – solidification temperature [°C]

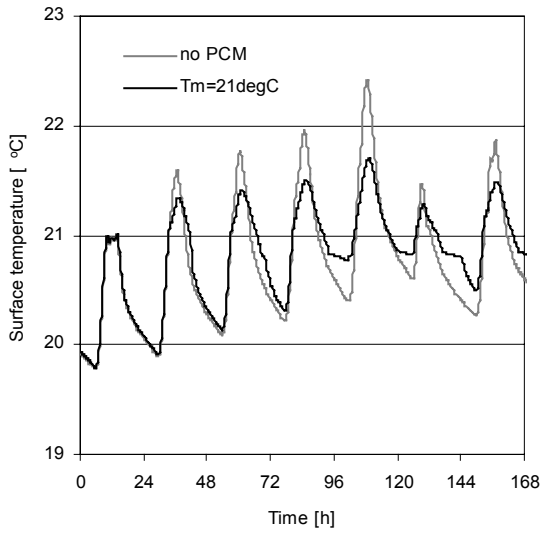


Figure 2. Wallboard surface temperature history with traditional (no PCM) and PCM ($T_m=21\text{ }^\circ\text{C}$).

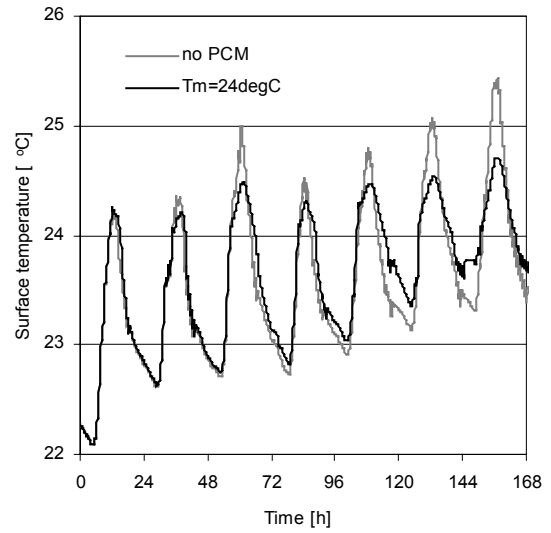


Figure 5. Wallboard surface temperature history with traditional (no PCM) and PCM ($T_m=24\text{ }^\circ\text{C}$).

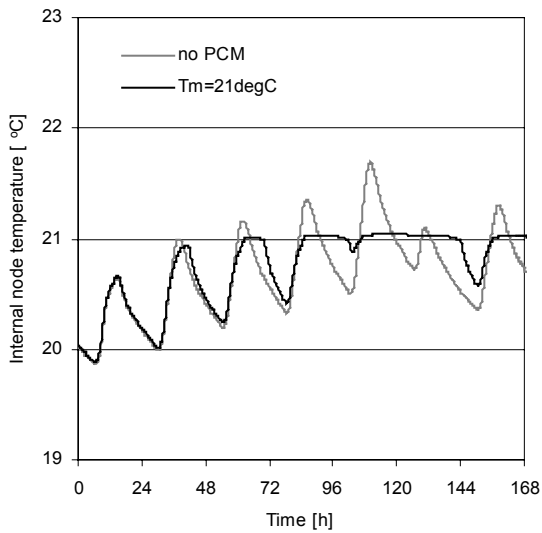


Figure 3. Internal node temperature history with traditional (no PCM) and PCM ($T_m=21\text{ }^\circ\text{C}$).

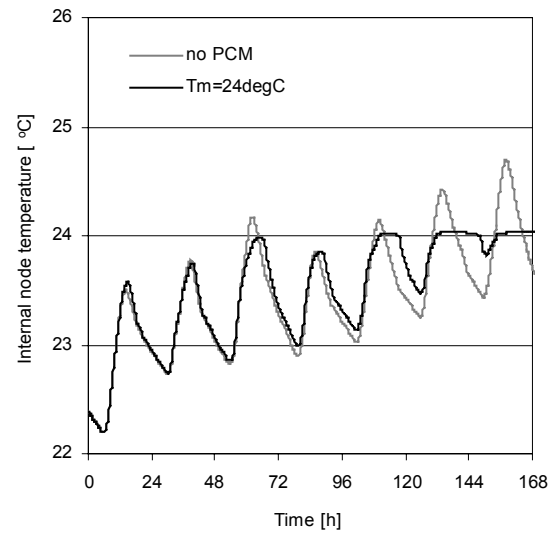


Figure 6. Internal node temperature history with traditional (no PCM) and PCM ($T_m=24\text{ }^\circ\text{C}$).

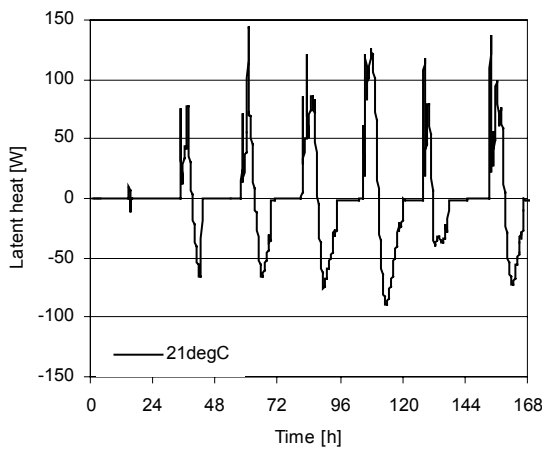


Figure 4. Solar energy stored as a latent heat in PCM-composite wallboard ($T_m=21\text{ }^\circ\text{C}$).

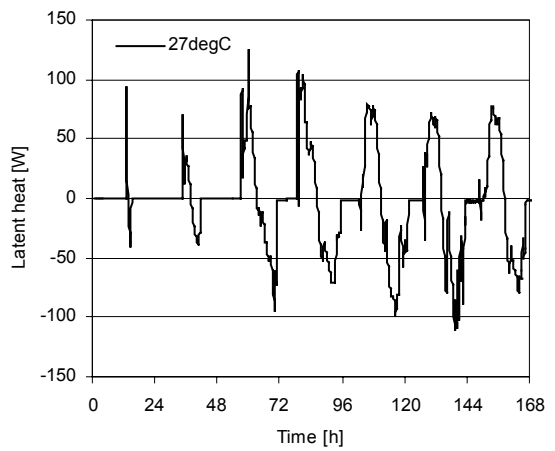


Figure 7. Solar energy stored as a latent heat in PCM-composite wallboard ($T_m=24\text{ }^\circ\text{C}$).

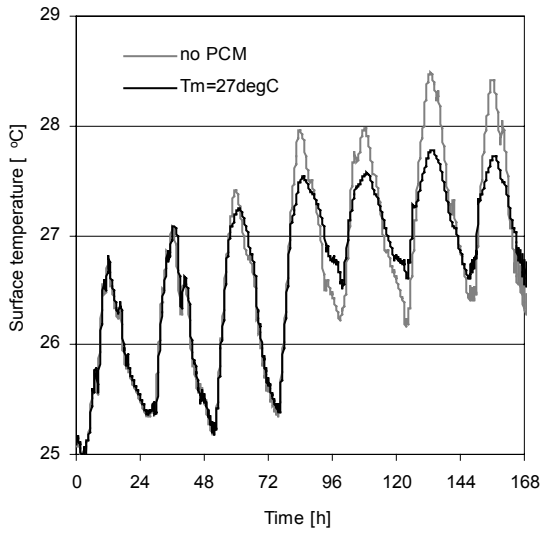


Figure 8. Wallboard surface temperature history with traditional (no PCM) and PCM ($T_m=27^\circ\text{C}$).

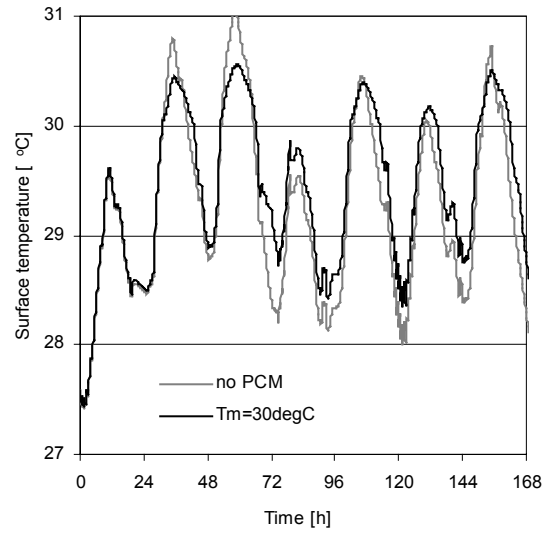


Figure 11. Wallboard surface temperature history with traditional (no PCM) and PCM ($T_m=30^\circ\text{C}$).

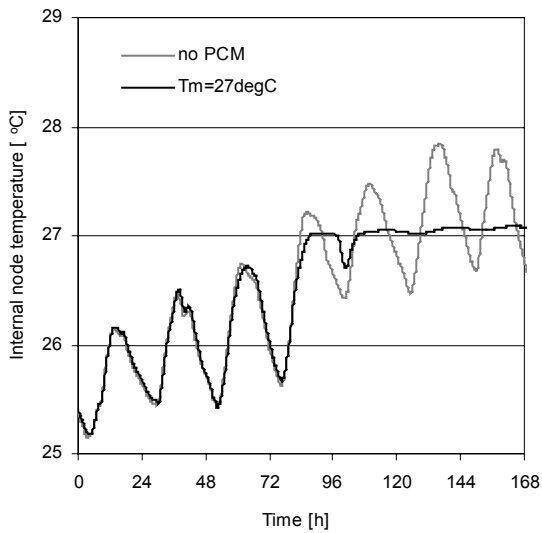


Figure 9. Internal node temperature history with traditional (no PCM) and PCM ($T_m=27^\circ\text{C}$).

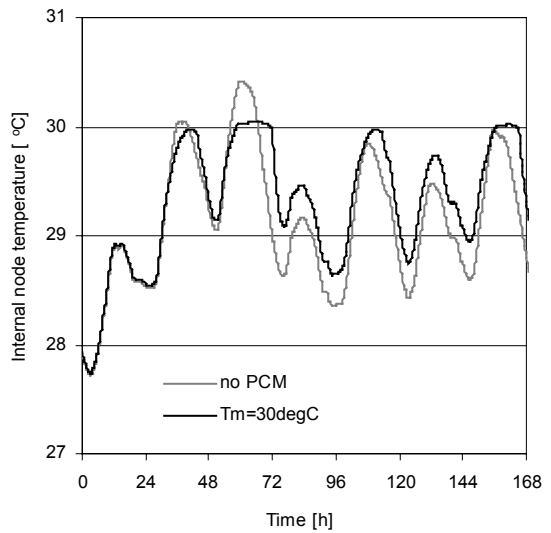


Figure 12. Internal node temperature history with traditional (no PCM) and PCM ($T_m=27^\circ\text{C}$).

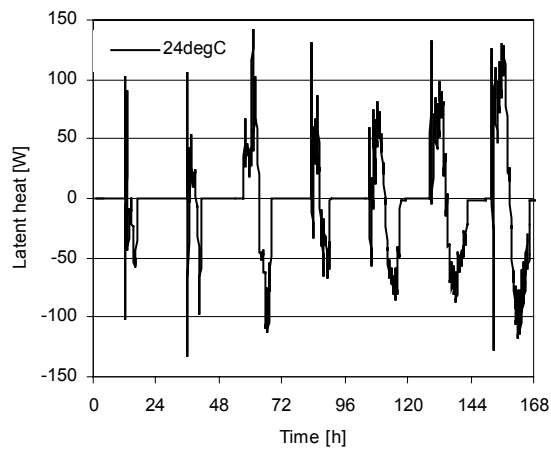


Figure 10. Solar energy stored as a latent heat in PCM-composite wallboard ($T_m=27^\circ\text{C}$).

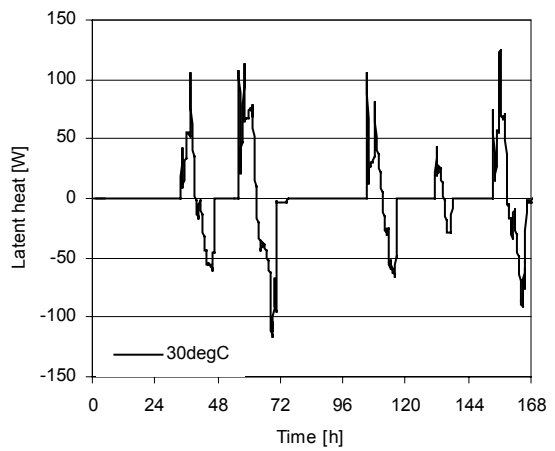


Figure 13. Solar energy stored as a latent heat in PCM-composite wallboard ($T_m=30^\circ\text{C}$).

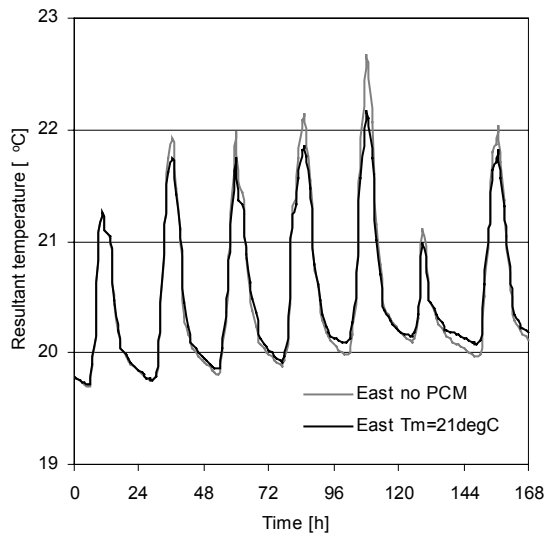


Figure 14. Resultant temperature history in east zone with traditional (no PCM) and PCM ($T_m=21\text{ }^\circ\text{C}$).

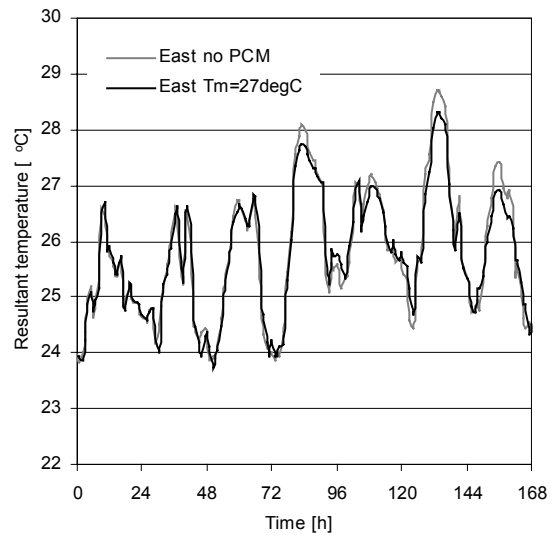


Figure 16. Resultant temperature history in east zone with traditional (no PCM) and PCM ($T_m=27\text{ }^\circ\text{C}$).

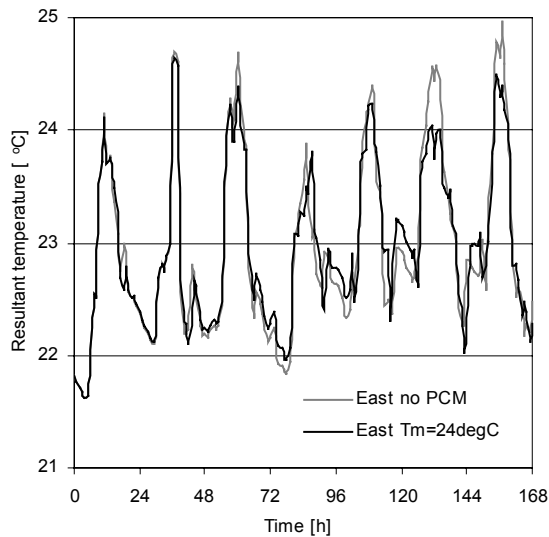


Figure 15. Resultant temperature history in east zone with traditional (no PCM) and PCM ($T_m=24\text{ }^\circ\text{C}$).

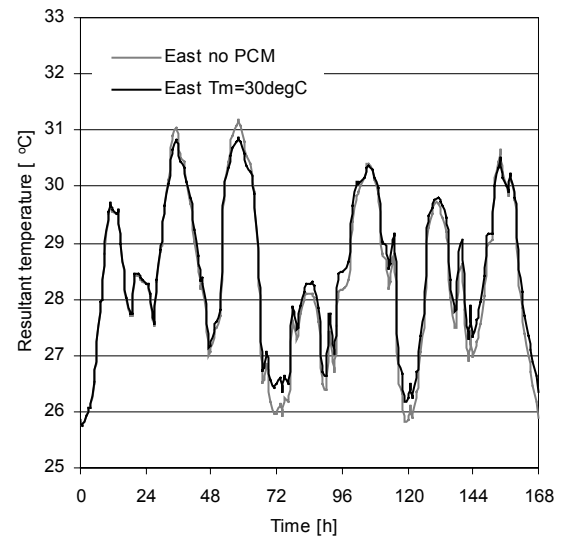


Figure 17. Resultant temperature history in east zone with traditional (no PCM) and PCM ($T_m=27\text{ }^\circ\text{C}$).

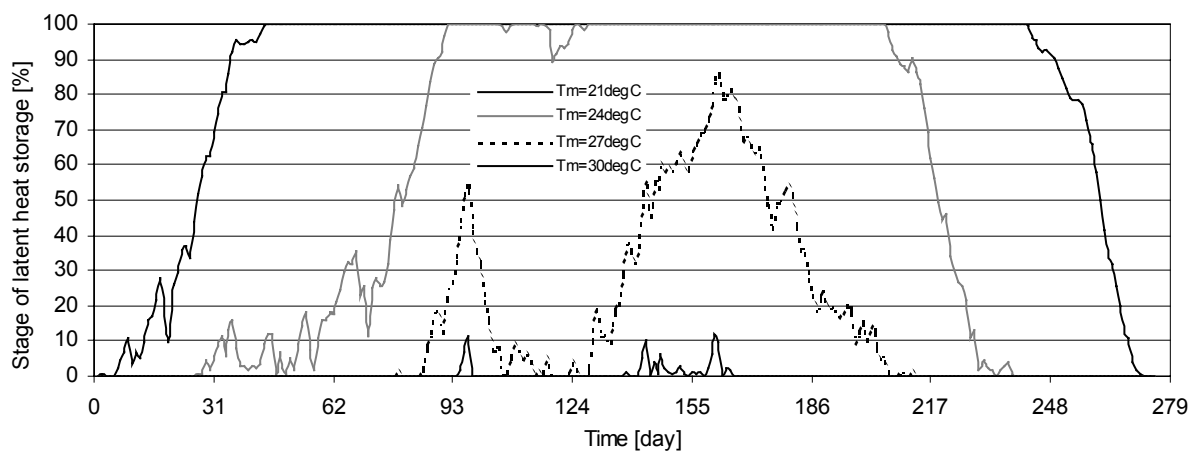


Figure 18. Latent heat storage stage for PCM-composites with different melting temperature from beginning of March to the end of November.